Bioorg. Med. Chem. 29 (2021) 115891

Contents lists available at ScienceDirect

Bioorganic & Medicinal Chemistry

journal homepage: www.elsevier.com/locate/bmc

Design, synthesis, and biological activity of novel semicarbazones as potent Ryanodine receptor1 inhibitors of Alzheimer's disease☆

Baozhu Dai [a,b], Xingxing Ma [a,b], Yadong Tang [a,b], Le Xu [a,b], Su Guo [a,b], Xinyan Chen [a,b], Shitong Lu [a,b], Guangjie Wang [a,b], Yajing Liu [a,b,*]

[a] Key Laboratory of Structure-Based Drug Design and Discovery (Shenyang Pharmaceutical University), Ministry of Education, 103 Wenhua Road, Shenhe District, Shenyang 110016, PR China

[b] Department of Pharmacology, Shenyang Pharmaceutical University, 103 Wenhua Road, Shenhe District, Shenyang 110016, PR China

ARTICLE INFO

Keywords:
RyR1 inhibitors
SOICR
Synthesis
Semicarbazones
AD

ABSTRACT

Ryanodine receptors (RyRs) are important ligand-gated Ca^{2+} channels; their excessive activation leads to Ca^{2+} leakage in the sarcoplasmic reticulum that may cause neurological diseases. In this study, three series of novel potent RyR1 inhibitors based on dantrolene and bearing semicarbazone and imidazolyl moieties were designed and synthesized, and their biological activity was evaluated. Using a single-cell calcium imaging method, the calcium overload inhibitory activities of 26 target compounds were tested in the R614C cell line, using dantrolene as a positive control. The preliminary investigation showed that compound 12a suppressed Ca^{2+} release as evidenced by store overload-induced Ca^{2+}release (SOICR) (31.5 ± 0.1%, 77.2 ± 0.1%, 93.7 ± 0.2%) at 0.1 μM, 3 μM and 10 μM, respectively. Docking simulation results showed that compound 12a could bind at the active site of the RyR1 protein. The Morris water-maze test showed that compound 12a significantly improved the cognitive behavior of AD-model mice. Further studies on the structural optimization of this series of derivatives are currently underway in our laboratory.

1. Introduction

Alzheimer's disease (AD) is a progressive neurodegenerative disease that is clinically characterized by dementia and neurobehavioral deterioration that seriously affects the quality of life and life expectancy. Approximately 30 million people have AD worldwide[1–3]. There is growing evidence that AD is a metabolic disorder due to a dysregulation in multiple biochemical pathways[4–7]. Furthermore, four main hypotheses have been intensively studied: the amyloid cascade hypothesis, tau hypothesis, metal ion (Ca^{2+}) hypothesis, and the cholinergic hypothesis. Currently, only six drugs have been approved: (i) the cholinesterase inhibitors: donepezil, rivastigmine, galantamine, and tacrine, (ii) the N-methyl-d-aspartate (NMDA) receptor antagonist memantine, and (iii) GV-971 that was approved in China in 2019.[8]

However, these drugs have limited therapeutic effects as they can only relieve the symptoms of AD and not stop or reverse the disease progression.[9,10] Studies have shown that the amyloid cascade, tau, and cholinergic hypotheses are related to Ca^{2+} homeostasis disorder.[11–17] Calcium ions play several roles in processes that are crucial for the functioning of neuronal cells, including membrane excitability and gene expression. Although dysregulation of intracellular Ca^{2+} and calcium homeostasis in cells of AD patients has been proposed as a common proximal cause of neurodegeneration in old age and Alzheimer's disease, much more attention has been focused on amyloid-β (Aβ) and tau as key causative factors for the disease. Nevertheless, there is accumulating evidence pointing to the importance of disturbed calcium signaling in AD pathogenesis.[18–20]

Ryanodine receptor (RyR) is a high-flux intracellular calcium channel that is responsible for the rapid and massive release of calcium into the cytoplasm from the sarcoplasmic reticulum (SR) or endoplasmic reticulum (ER).[21–23] This process plays an indispensable role in many cellular functions. Over-activation of the RyR channel causes leakage of Ca^{2+} from the SR store.

Dantrolene (Fig. 1), a small-molecule RyRs antagonist, was used for

☆ In this study, three series of novel potent RyR1 inhibitors bearing semicarbazones and imidazoles moiety based on dantrolene were designed, synthesized and evaluated for their biological activity, and compound 12a could improve the cognitive state in Mirror water maze test on AD mouse model.

* Corresponding author at: Key Laboratory of Structure-Based Drug Design and Discovery (Shenyang Pharmaceutical University), Ministry of Education, 103 Wenhua Road, Shenhe District, Shenyang 110016, PR China.

E-mail address: lyjpharm@126.com (Y. Liu).

https://doi.org/10.1016/j.bmc.2020.115891
Received 20 August 2020; Received in revised form 18 November 2020; Accepted 19 November 2020
Available online 26 November 2020

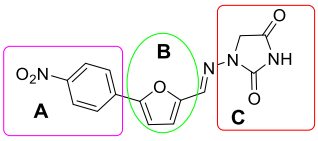

Fig. 1. . Dantrolene.

the treatment of malignant hyperthermia (MH).[24] Because of its involvement in calcium homeostasis, dantrolene has been investigated for its potential as a neuroprotective in several animal models of AD.[25] RyRs channels govern the process of spontaneous Ca^{2+} release from Ca^{2+}-overload SR known as the store overload-induced Ca^{2+} release (SOICR). Chen et al.[26] reported that dantrolene could directly interact with RyR1 and inhibit the release of calcium from the ER and SR to reduce intracellular calcium overload.[27] Furthermore, they discovered that dantrolene could inhibit SOICR potently in HEK293 cells expressing RyR1 but not RyR2. Therefore, we selected the RyR1 cell line R614C to evaluate the activity of our compound *in vitro*. Peng et al. reported that memory consolidation and working memory in 3xTg-AD mice were significantly improved by treatment with dantrolene.[28] Chakroborty et al. found that Aβ deposition within the cortex and hippocampus was reduced after the short-term administration of dantrolene in AD model mice.[29] Unfortunately, dantrolene has many adverse reactions, such as muscle weakness, phlebitis, respiratory failure, and gastrointestinal symptoms.[30] Therefore, we used dantrolene as the lead compound and introduced a structural modification to obtain candidate compounds with fewer side effects and higher calcium inhibition.

The challenge in the treatment of central nervous system diseases is mainly the inability of the drug to penetrate the blood–brain barrier (BBB).[31] In this study, we modified the lead compound by opening the hydantoin ring and removing the acetyl group to form an acylhydrazide structure. To increase the lipid solubility of dantrolene derivatives, phenyl or benzyl substituents were added to the terminal N atom to obtain two series of new compounds. Another series of derivatives were generated by replacing phenyl with imidazolyl, expecting that compounds with imidazolyl groups would have better aqueous solubility and binding affinity.

Consequently, a 5-(4-nitrophenyl) furan-2-methylene amino fragment was retained, substituted phenyl or benzyl groups were introduced into the terminal N atom of the hydantoin ring to obtain Series I and II of candidate compounds. Series III of imidazole derivatives was designed to improve the compounds' aqueous solubility (Fig. 2).

2. Results and discussion

2.1. Chemistry

2.1.1. Synthesis of target compounds 6a-6l, 10a-10j, 12a-12d

The general routes of synthesis for the target compounds are illustrated in Schemes 1–5. Commercially available 4-nitroaniline was treated with $NaNO_2$/HCl to obtain the diazonium derivative (**1**) that was condensed with furan-2-carbaldehyde in the presence of copper chloride to provide the key intermediate 5-(4-nitrophenyl) furan-2-carbaldehyde (**2**).

Intermediates **5a-5l** were synthesized as outlined in Scheme 2. The substituted aniline was reacted with phenyl carbonochloridate to obtain intermediates **4a-4l** that were treated with hydrazine hydrate to obtain intermediates **5a-5l**. The synthesis method of **9a-9j** was the same as that of **5a-5l** outlined in Scheme 3. The intermediates **11a-11d** were synthesized as profiled in Scheme 4. The substituted ethyl ester was treated with hydrazine hydrate to obtain intermediates **11a-11d**

As described in Scheme 5, intermediates **2** were treated with intermediates **5a-5l**, **9a-9j** or **11a-11d** to afford the target compounds, respectively.

2.2. Biological evaluation

2.2.1. Biological activity of dantrolene derivatives

R614C cells express RyR1-R614C mutation. Single-cell calcium imaging can be used to monitor changes in calcium ions in the cytoplasm. Dantrolene was used as a positive control and DMSO as a blank control. Different concentrations of the target compounds (0.1 μM, 3μM, 10 μM) were used to evaluate the inhibitory activity on calcium channels *in vitro*. The inhibition rate (%) of SOICR was used to characterize the activity of the compounds and is shown in Table 1 as an average value obtained from at least three independent experiments.

2.2.2. In vitro SOICR inhibition activities and SARs study

As shown in Table 1, most of the target compounds exhibited

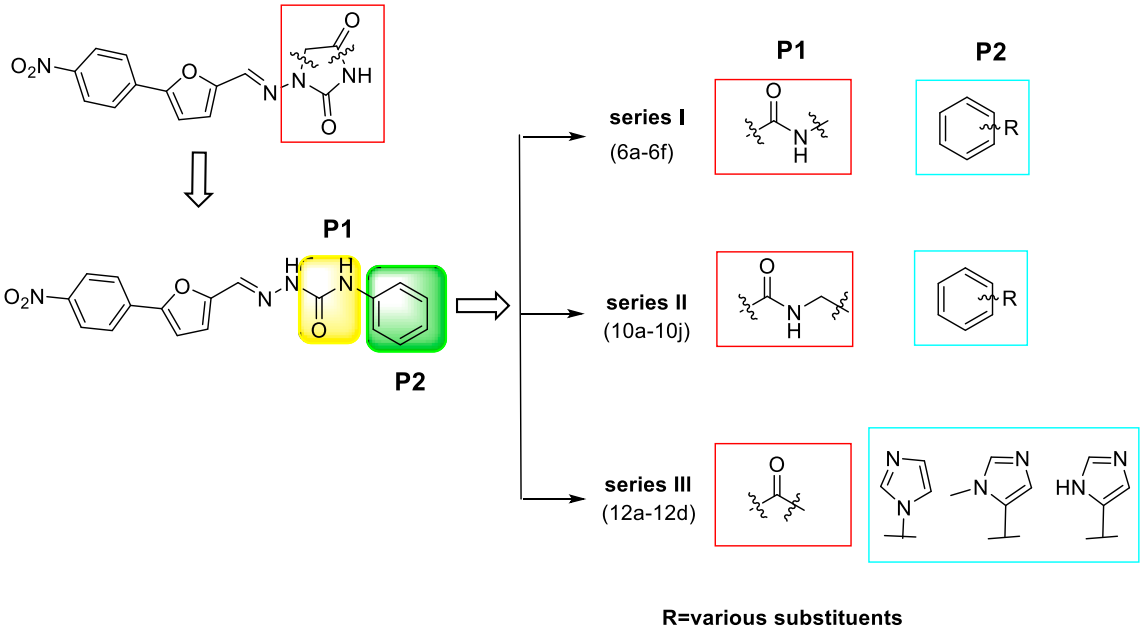

Fig. 2. . Design strategy for the dantrolene derivatives.

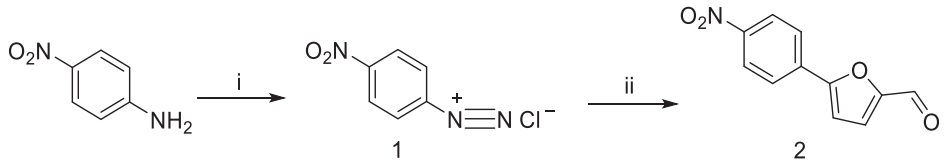

Scheme 1. Reagents and conditions: (i): 20%HCl, $NaNO_2$, 0℃, 30 min; (ii): furan-2-carbaldehyde, $CuCl_2{\cdot}H_2O$ acetone, 0℃, 6 h.

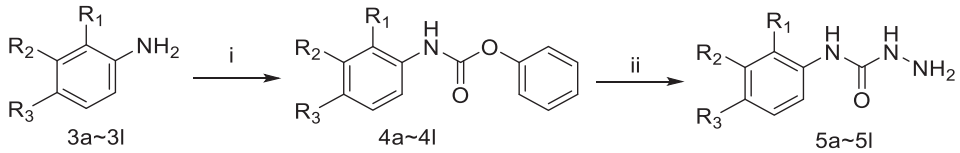

Scheme 2. Reagents and conditions: (i): phenyl carbonochloridate; Na_2CO_3, THF: EA: H_2O = 1:3:1, 25℃, 6 h; (ii): $NH_2NH_2{\cdot}H_2O$ (80%), EtOH, rt, 4 h.

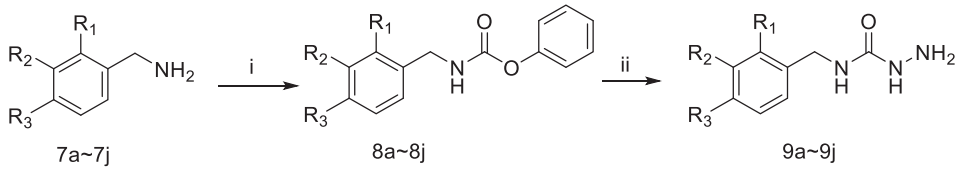

Scheme 3. Reagents and conditions: (i): phenyl carbonochloridate; Na_2CO_3, THF: EA: H_2O = 1:3:1,25℃,4h; (ii): $NH_2NH_2{\cdot}H_2O$ (80%), EtOH, rt, 3 h.

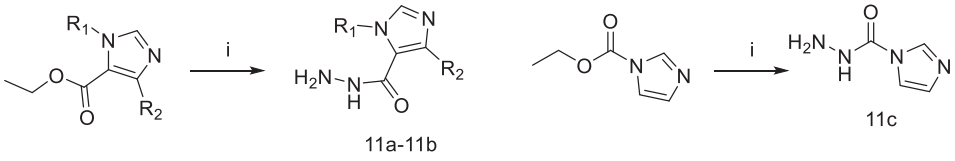

Scheme 4. Reagents and conditions: $NH_2NH_2{\cdot}H_2O$ (80%), EtOH, rt, 3 h.

moderate or excellent inhibitory activity against SOICR at different concentrations (0.1 μM, 3 μM and 10 μM). Activities of compounds 6a (15.90 ± 0.3%, 35.8 ± 0.2%, 93.9 ± 2.3%), 10e (23.6 ± 0.3%, 35.1 ± 0.1%, 76.1 ± 0.1%) and 12a (31.5 ± 0.1%, 77.2 ± 0.1%, 93.7 ± 0.2%) were equivalent to those of dantrolene (30.8 ± 0.1%,73.1 ± 0.1%,94.2 ± 0.2%). Compound 12a was the best candidate and markedly suppressed Ca^{2+} oscillations. The study has shown that these compounds inhibit SOICR in a dose-dependent manner; we will discuss the structure–activity relationship at 10 μM.

The inhibitory effect of the target compounds and dantrolene on SOICR in R614C cells is shown in Table 1. Phenyl- and benzyl-substituted derivatives had a similar effect at different concentrations. The imidazole derivatives were more potent.

Phenyl derivatives (Series I) containing electron-withdrawing groups (EWG) on the benzene ring, such as bromine (6e) and chlorine (6 h), showed higher activities than compounds containing electron-donating groups (EDG), such as methyl (6d) and methoxy (6i). Furthermore, the activity of meta-substituted derivatives was better than the activity of substituted derivatives at other sites (6c *vs* 6f). Unexpectedly, compound 6a with no phenyl substitution was more potent than those with a substituted phenyl group.

Similar biological properties were observed for the benzyl derivatives (Series II). Compounds with EWG suppressed SOICR better than those with EDG in the benzene ring. For example, the activities of compounds 10b (4-Cl, 70.4 ± 0.1%), 10e (4-F, 76.1 ± 0.1%), and 10i (4-CF_3, 53.1 ± 0.3%) were better than that of compound 10j (4-CH_3, 35.4 ± 0.3%). However, the substitution position also affected the activity, with para-substitution being more beneficial than the other two sites as seen in compounds 10e (4-F, 76.1 ± 0.1%) *vs* 10c (2-F, 44.6 ± 0.1%) and 10d (3-F, 72.1 ± 0.2%). Compared with monosubstituted compounds, the activity of disubstituted compounds was significantly lower, such as for 10b compared to 10f–10h.

Although compound 6a showed high inhibitory activity, its water solubility was poor. Therefore, we replaced the phenyl with imidazolyl to improve water solubility hoping that it would enhance the interaction between the target compound and the receptor. Compounds 12a-12d contain different substituents on the imidazole ring and amide nitrogen atom. Fortunately, compound 12a showed the same activity as dantrolene and its solubility was better than that of dantrolene and phenyl derivatives; it is currently the best candidate compound. For compounds 12c, 12b, and 12d, the introduction of methyl groups into the imidazole ring and amide nitrogen atom decreased slightly the compounds' activity.

2.2.3. The activities of the target compounds inhibiting AChE

It has been reported that dantrolene can inhibit AChE,[32,33] so we used donepezil as a positive control to test the effect of dantrolene and its derivatives on AChE. The effects of dantrolene, six synthesized compounds (6a, 6b, 10d, 10 g, 12a, and 12b), and donepezil (positive control) on AChE activity were determined using the Ellman method[34] via the use of a sodium phosphate buffer (pH 8.0), with either the absence or presence of the abovementioned compounds. First, we measured the enzyme inhibition rate of compounds at a fixed concentration of 5.0 μM against AChE, as summarized in Table 2. Dantrolene and dantrolene derivatives 10d, 12a, and 12b showed weak AChE inhibitory activity, while 6a, 6b, and 10g showed moderate AChE inhibitory activity. The positive control compound, donepezil, significantly inhibited AChE activity.

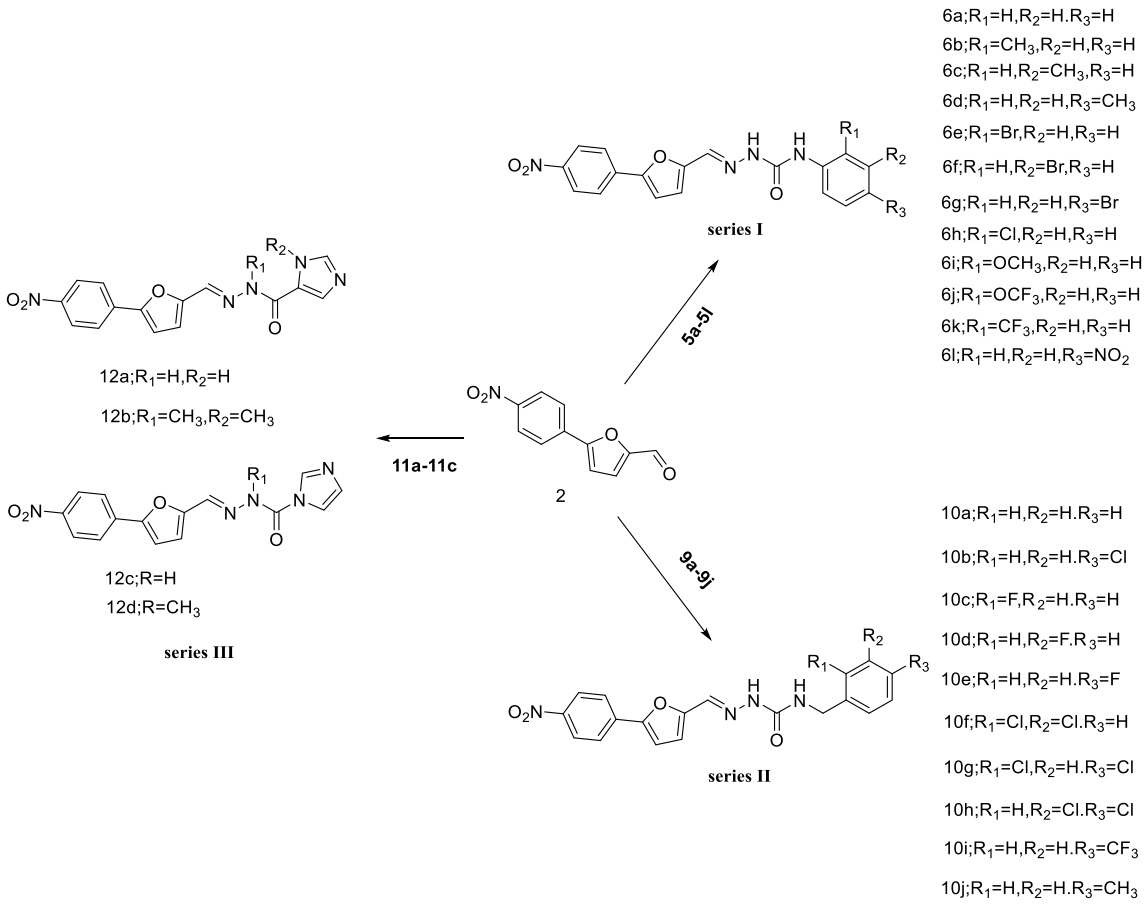

Scheme 5. Reagents and conditions: EtOH, AcOH, rf, 2 h.

2.2.4. *Kinetic water solubility*

In order to compare the solubility difference between terminal benzene ring and imidazolyl, we tested kinetic water solubility of dantrolene and its derivatives 6a, 12a and 12b. We determined the kinetic water solubility of 12a using a standard turbidimetric assay and compared this with those of 6a and dantrolene. The aqueous solubilities of 12a improved in comparison to 6a and dantrolene (Table 3). The compound 12a exhibited the best kinetic water solubility (9-fold greater than 6a, and similar to those of dantrolene and 12b), demonstrating the introduction of an imidazolyl group at the end of the carbonyl group to be a feasible solution to improve water solubility.

2.2.5. *Binding model analysis*

Based on the *in vitro* pharmacological results, we selected compound 12a, the best RyR1 inhibitor in this study, as the docking model (PDB ID:6M7H). As shown in Fig. 3(A), ASP80 forms a hydrogen bond between the nitrogen atoms of imidazole and amide. The following reciprocity mutual effect was noted: (1) one pi-alkyl interaction between the imidazole ring and residue LYS75; (2) two pi-sigma interactions between the benzene ring and residue MSE71 and LEU32, respectively; (3) one carbon-hydrogen interaction between a carbon atom of the imidazole ring and residue LYS75. The 3D model of the interactions between compound 12a and the protein crystal structure shown in Fig. 3(B) indicated that the active pockets were occupied by compound 12a.

The optimum cLogP value and molecular weight of the drug passing through the blood–brain barrier are 2.8 and 305.3, respectively[35]. Some physicochemical properties of the target compounds and dantrolene were predicted using the free online website (http://www.molinspiration.com) for their adaptability with Lipinski's rule of five and the best value of passing through the blood–brain barrier. As shown in Table 4, compounds 6d, 6f, and 12a were better than dantrolene, and 12a exhibited the best drug-like properties.Table5 (see Table 6).

2.2.6. *In vivo test*

Behavioral test: Morris water maze test was used to evaluate the spatial learning and memory ability of the animal model. In this experiment, SPF grade FAD mice were administered at the age of 5 months, male and female at random, and the test began 30 days after administration.[36] The mice were divided into two groups: The test group was intraperitoneally injected at a dose of 3.2 mg/kg with 12a DMSO solution (1.12 mg/mL), and the control group was intraperitoneally injected with a same volume of DMSO.

The results were presented in Figure 4, and the statistical significance of each was analyzed by ANOVA versus the DMSO and compound 12a groups. As shown in Fig. 4B, the administration of compound 12a during the drug treatment period (30 consecutive days) did not influence the mean daily bodyweight profile of mice. This suggested that long-term administration of compound 12a is safe at doses of 3.2 mg/kg/day. During the training trials, the mean escape latency for the mice in the 12a group declined progressively compared with those in the DMSO group (Day 2, 29.89 s *vs* 36.72 s, $p < 0.05$; Day 3, 25.12 s *vs* 35.59 s, $p < 0.05$; Day 4, 16.23 s *vs* 31.99 s, $p < 0.001$) (Fig. 4C). Memory retention was assessed by performing a spatial memory probe trial with the platform removed from the pool 24 h after the last training trial. The results of Fig. 4D showed that the percentage of swimming time on target zone (southwest quadrant) in compound 12a group (35.7 ± 1.2) was significantly higher than that in DMSO group (23.1 ± 1.1), which indicated that the cognitive and memory functions of FAD mice in compound 12a group were improved more obviously on the dosage of 3.2 mg/Kg/day (see Fig 5).

Table 1
The activities of the target compounds inhibiting Ca^{2+}.

Compd.	R	SOICR Inhibition (%) (Mean ± SD[a], N = 3)		
		0.1 μM[b]	3 μM[b]	10 μM[b]
6a	H	15.90 ± 0.3	35.8 ± 0.2	93.9 ± 2.3
6b	2-CH_3	-[c]	–	–
6c	3-CH_3	10.7 ± 0.1	15.2 ± 0.1	34.6 ± 0.1
6d	4-CH_3	–	10.8 ± 0.1	29.5 ± 0.1
6e	2-Br	20.1 ± 0.1	38.5 ± 0.2	67.1 ± 0.1
6f	3-Br	26.7 ± 0.4	67.1 ± 0.1	67.1 ± 0.1
6g	4-Br	13.2 ± 0.2	31.3 ± 0.2	52.9 ± 0.2
6h	2-Cl	–	25.1 ± 0.2	50.1 ± 0.1
6i	2-OCH_3	–	–	30.6 ± 0.1
6j	2-OCF_3	–	20.4 ± 0.2	57.1 ± 0.1
6k	2-CF_3	12.6 ± 0.2	30.1 ± 0.1	55.5 ± 0.1
6l	4-NO_2	–	14.1 ± 0.2	32 ± 0.1
10a	H	–	23.1 ± 0.3	48.6 ± 0.1
10b	4-Cl	27.1 ± 0.3	48.6 ± 0.1	70.4 ± 0.1
10c	2-F	–	26.1 ± 0.1	44.6 ± 0.1
10d	3-F	–	25.8 ± 0.3	72.1 ± 0.2
10e	4-F	23.6 ± 0.3	35.1 ± 0.1	76.1 ± 0.1
10f	2,3-$(Cl)_2$	–	–	30.6 ± 0.1
10g	2,4-$(Cl)_2$	–	–	16.2 ± 0.2
10h	3,4-$(Cl)_2$	–	25.3 ± 0.2	37.2 ± 0.1
10i	4-CF_3	19.7 ± 0.2	27.9 ± 0.3	53.1 ± 0.3
10j	4-CH_3	–	–	35.4 ± 0.3
12a	R_1 = H; R_2 = H	31.5 ± 0.1	77.2 ± 0.1	93.7 ± 0.2
12b	R_1 = CH_3;R_2 = CH_3	24.5 ± 0.3	70.5 ± 0.3	82.5 ± 0.1
12c	H	26.1 ± 0.2	48.4 ± 0.3	68.2 ± 0.1
12d	CH_3	23 ± 0.2	53.5 ± 0.1	74.9 ± 0.2
DMSO[d]		–	–	–
Dantrolene[e]		30.8 ± 0.1	73.1 ± 0.1	94.2 ± 0.2

[a] Standard deviation.
[b] The concentration of the compound.
[c] Means no activity at the concentration.
[d] Used as a blank control.
[e] Used as a positive control.

Table 2
Effects of dantrolene derivatives 6a, 6b, 10d, 10 g, 12a, and 12b on AChE inhibition.

Compd.	AChE Inhibition (%)[a] (Mean ± SD[b], N = 3)
6a	19.3 ± 2.56
6b	18.2 ± 3.19
10d	33.6 ± 1.09
10g	8.9 ± 3.45
12a	24.8 ± 0.64
12b	14.3 ± 2.1
Donepezil	99.4 ± 0.23[c]
Dantrolene	0.1 ± 2.5

[a] At 5.0 μM.
[b] Standard deviation.
[c] At 1.0 μM.

Table 3
Kinetic water solubility of dantrolene, 6a, 12a, and 12b.

Compound	Solubility limit [a,b,c](mM)
Dantrolene	0.56
6a	0.06
12a	0.58
12b	0.48

[a] Precipitation was determined by turbidity at 540 nm.
[b] Absorbance value > "mean + 3 standard deviations" from the blank was considered turbid.
[c] The coefficient of variation (CV) was < 1.5% for all four compounds.

3. Conclusions

In this study, three series of novel potent RyR1 inhibitors based on dantrolene and bearing semicarbazone and imidazole moieties were designed, synthesized, and evaluated for their biological activity. The results of pharmacological experiments showed that several of the new compounds (6a, 6e, 10d, 10e, 12a, 12b) had moderate to excellent ability to suppress SOICR in R614C cells *in vitro*. The primary SARs showed that the opening of the hydantoin ring of the lead compound could retain activity and especially the introduction of hydrophilic imidazolyl group could improve the affinity of RyR1. Fortunately, imidazolyl derivative 12a exhibited the best potency *in vitro* with SOICR inhibition of 31.5 ± 0.1% at a concentration of 0.1 μM. Although 12a inhibited the activity of AChE, it was much weaker than donepezil. Furthermore, the Morris water-maze test provided evidence that compound 12a could significantly improve the cognitive behavior of AD-model mice. The docking simulation results showed that compound 12a could bind well at the active site of RyR1, with imidazole providing a much more suitable size for occupying the hydrophobic cavity compared with dantrolene. Further studies on the structural optimization of this series of derivatives are currently underway in our laboratory.

4. Experimental

4.1. Chemistry

Unless otherwise specified, all materials were obtained from commercial suppliers and were used without further purification. Reactions' time and purity of the products were monitored by TLC on FLUKA silica gel aluminum cards (0.2 mm thickness) with fluorescent indicator 254 nm. Column chromatography was run on silica gel (200–300 mesh) from Qingdao Ocean Chemicals (Qingdao, Shandong, China). All melting points were obtained on a Büchi Melting Point B-540 apparatus (Büchi Labortechnik, Flawil, Switzerland) and were uncorrected. Mass spectra (MS) were taken in ESI mode on Agilent 1100 LC–MS (Agilent, Palo Alto, CA, USA). ^{1}H NMR and ^{13}C NMR spectra were recorded on Bruker ARX-400, 400 MHz spectrometers (Bruker Bioscience, Billerica, MA, USA) with TMS as an internal standard.

4.1.1. Preparation of 5-(4-nitrophenyl) furan-2-carbaldehyde (2)

4.1.1.1. Preparation of 1-chloro-2-(4-nitrophenyl) diazo salt (1). To a suspension of finely powdered p-nitroaniline (2.54 g, 20 mmol) in 10 mL of 24% aq hydrochloric acid at 0 °C was added a cold aqueous solution of sodium nitrite (1.7 g, 23 mmol), and the reaction mixture was stirred for 1 h at 0–5 °C to obtain 4-nitrobenzenediazonium chloride (1). The reaction solution of diazonium salt 1 was directly used for the next reaction.

4.1.1.2. Preparation of 5-(4-nitrophenyl) furan-2-carbaldehyde (2). 4-Nitrobenzenediazonium Chloride (1) was added dropwise under stirring to a solution of furfural (0.1 mol, 9.6 g) and $CuCl_2{\cdot}2H_2O$ (0.058 mol, 1 g) in acetone (40 mL) at 20–30 °C. The mixture was stirred until nitrogen no longer evolved, diluted with water (200 mL), and filtered to yield 5-(4-nitrophenyl) furan-2-carbaldehyde (2), which was recrystallized from DMF (17.7 g, 81.7%). Mp:202.7–204.1 °C, MS (ESI) *m/z* (%): 218.26 $[M+H]^+$; ^{1}H NMR (400 MHz, DMSO-d_6) δ (ppm): 9.69 (s, 1H, CHO), 8.35 (d, J = 8.9 Hz, 2H, Ph-H), 8.13(d, J = 8.9 Hz, 2H, Ph-H), 7.72 (d, J = 3.8 Hz, 1H, furan-H), 7.59 (d, J = 3.8 Hz, 1H, furan-H).

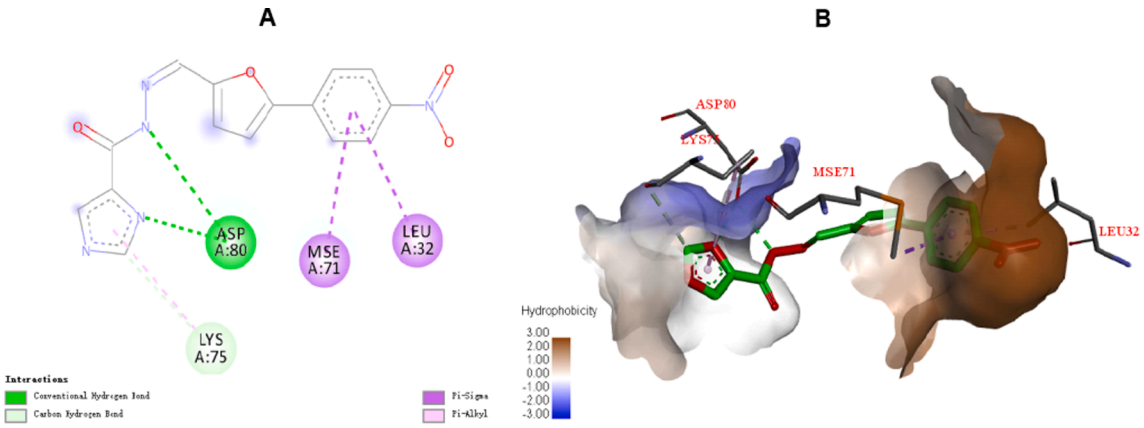

Fig. 3. . Docking mode of compound **12a**. (A) 2D molecular docking model of compound **12a**. (B) 3D interaction map between compound **12a** and binding sites.

Table 4
Prediction of physicochemical properties[a] of the target compounds.

Compd	miLogP	TPSA	natoms	MW	nON	nOHNH	nviolations	nrotb	volume
Standard	<5	<140		<500	<5	<5		≤10	
6d	**4.7**	**112.5**	**28**	**378.69**	**8**	**2**	**0**	**6**	**332.17**
6f	4.84	112.5	28	443.26	8	2	1	6	333.5
12a	**2.46**	**129.11**	**24**	**325.28**	**9**	**2**	**0**	**5**	**267.24**
Dantrolene[b]	1.75	120.7	23	314.26	9	1	0	4	252.73

[a] miLogP: molinspiration predicted Log P; TPSA: topological polar surface area; natoms: no. of atoms; MW: molecular weight; nON: no. of hydrogen bond acceptors; nOHNH: no. of hydrogen bond donors; nviolations: no. of violations; nrotb: no. of rotatable bonds; volume: molar volume.
[b] Used as positive control.

Table5
The single-cell Ca^{2+} imaging time.

Ca^{2+} con.	Drug con.	Caffeine con.	Time (min)	End point in time (s)
0	0	0	3	180
0.1 mM	0	0	3	360
0.5 mM	0	0	3	540
1 mM	0	0	8	1020
1 mM	0.1 μM	0	8	1500
1 mM	3 μM	0	8	1980
1 mM	10 μM	0	8	2460
1 mM	0	10 mM	3	

Table 6
Mirror water maze protocol*.[36]

	Day 1	Day 2	Day 3	Day 4	Day 5
	Platform Location: SW Starting Location as follows:				No platform.
Trial 1	W	N	N	E	N
Trial 2	S	W	E	S	
Trial 3	N	E	W	W	
Trial 4	E	W	S	E	
Trial 5	S	S	N	N	

* On days 1–4, the platform position remains constant while the starting direction changes. On day 5, there is no platform and a single trial. The starting direction for day 5 is farthest from the previous platform location (N) so that the mice must travel some distance before entering the previously learned platform quadrant.

*4.1.2. General procedure for preparation of acylhydrazine intermediates (**5a-5l, 9a-9j**)*

*4.1.2.1. General procedure for preparation of different substitution phenyl phenylcarbamate (**4a-4l**).* 3 μmol substituted aniline and Na_2CO_3 (0.19 g, 1.8 μmol) were dissolved in the solution of 10 mL (THF: EA: H_2O = 1:3:1) and stirred at 25°C for 15 min, then phenyl chloroformate (0.499 g, 3.2 μmol) was dropped to the reaction solution at room temperature, stirred for 6 h. When TLC showed the completion of the reaction, the resulting precipitate was filtered, washed with H_2O and dried under reduced pressure to obtain the title compound*(**4a-4l**)*.

*4.1.2.2. Phenyl phenylcarbamate (**4a**).* Yellowish solid; Yield: 78.4.0%. MS (ESI) *m/z* (%): 214.3 $[M+H]^+$.

*4.1.2.3. Phenyl o-tolylcarbamate (**4b**).* Yellow solid; Yield: 67.8%. MS (ESI) *m/z* (%): 228.2 $[M+H]^+$.

*4.1.2.4. Phenyl m-tolylcarbamate (**4c**).* Yellowish solid; Yield: 72.6%. MS (ESI) *m/z* (%): 228.2 $[M+H]^+$.

*4.1.2.5. Phenyl p-tolylcarbamate (**4d**).* Dark yellow solid; Yield: 65.6%. MS (ESI) *m/z* (%): 228.2 $[M+H]^+$.

*4.1.2.6. Phenyl (2-bromophenyl)carbamate (**4e**).* Brown-black solid ; Yield: 64.2%. MS (ESI) *m/z* (%): 293.2 $[M+H]^+$.

*4.1.2.7. Phenyl (3-bromophenyl)carbamate (**4f**).* Brown solid; Yield: 61.3%. MS (ESI) *m/z* (%): 293.2 $[M+H]^+$.

*4.1.2.8. Phenyl (4-bromophenyl)carbamate (**4g**).* Yellowish brown solid; Yield: 72.2%. MS (ESI) *m/z* (%): 293.2 $[M+H]^+$.

*4.1.2.9. Phenyl (2-chlorophenyl)carbamate (**4h**).* Yellowish solid; Yield: 65.2%. MS (ESI) *m/z* (%): 248.8 $[M+H]^+$.

*4.1.2.10. Phenyl (2-methoxyphenyl)carbamate (**4i**).* Milky yellow solid; Yield: 67.6%. MS (ESI) *m/z* (%): 244.2 $[M+H]^+$.

*4.1.2.11. Phenyl (2-(trifluoromethoxy)phenyl)carbamate (**4j**).* Yellow solid; Yield: 62.2%. MS (ESI) *m/z* (%): 298.3 $[M+H]^+$.

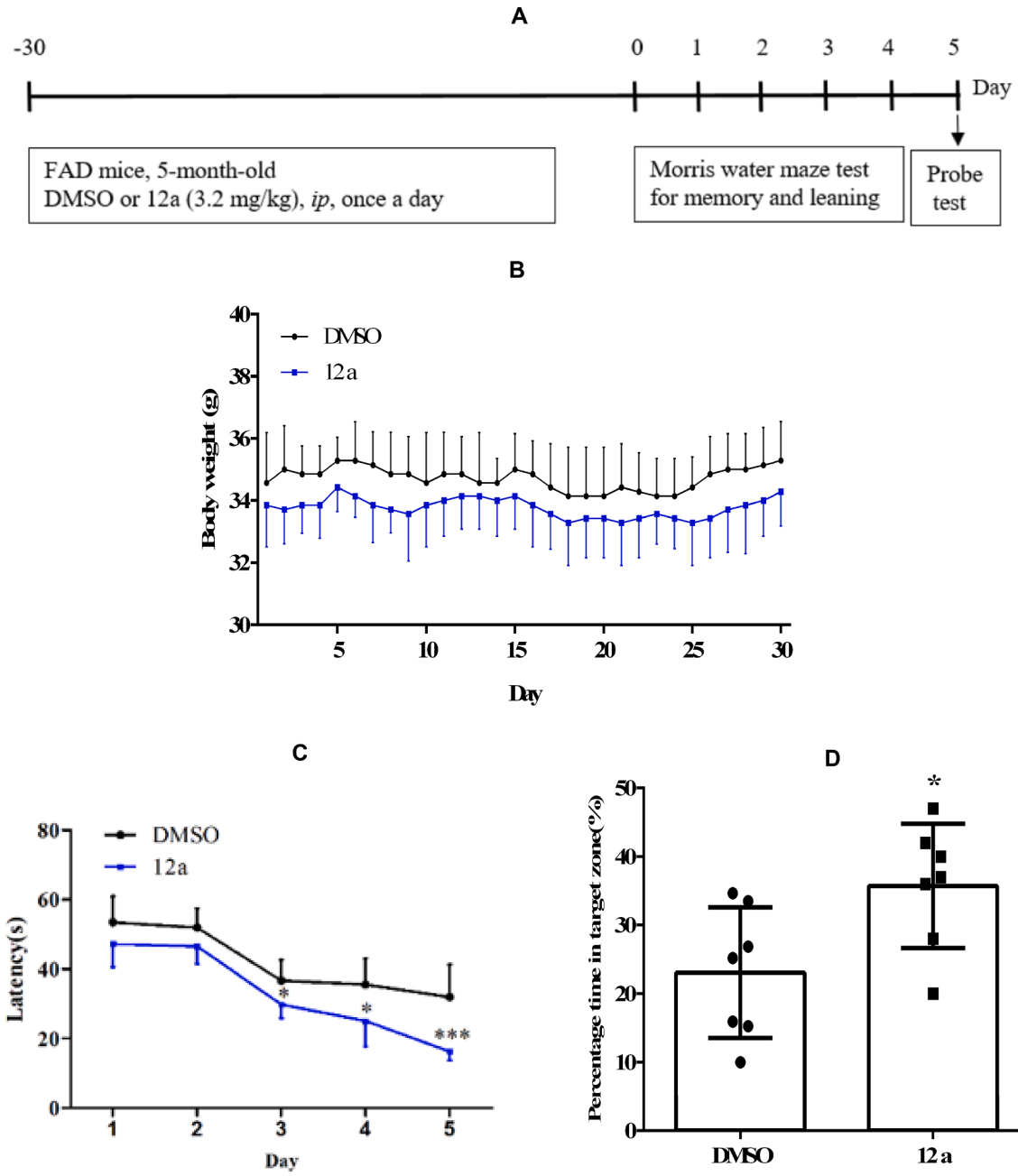

Fig 4. Memory and learning were tested using the Morris water maze. (A) Timeline for 12a treatment and behavioral assessment. (B) Average body weight of the mice measured daily during the administration. Data were expressed as means ± standard deviations (n = 7). Compound 12a treatment blocks memory loss in 5-month-old FAD mice. Memory and learning were tested using the Morris water maze. (C) The mean escape latency over four consecutive days of reference memory testing. Data are expressed as means ± standard deviations (n = 7). $^{*}p < 0.05$ and $^{***}p < 0.001$, compared with the DMSO group. (D) A probe test was performed 24 h after the last training trial to determine memory retention. Data were expressed as means ± standard deviations (n = 7). $^{*}p < 0.05$, compared with the DMSO group.

*4.1.2.12. Phenyl (2-(trifluoromethyl)phenyl)carbamate (**4k**).* Yellowish solid; Yield: 72.6%. MS (ESI) *m/z* (%): 282.3 $[M+H]^+$.

*4.1.2.13. Phenyl (4-nitrophenyl)carbamate (**4l**).* Dark green solid; Yield: 65.6%. MS (ESI) *m/z* (%): 259.2 $[M+H]^+$.

*4.1.3. General procedure for preparation of different substitution phenyl benzylcarbamate (**8a-8j**)*

The preparation of the key intermediate **8a-8j** is the same as way to preparation **4a-4l**, So the synthesis method would not be listed here.

*4.1.3.1. Phenyl benzylcarbamate (**8a**).* Yellow solid; Yield: 71.2%. MS (ESI) *m/z* (%): 228.4 $[M+H]^+$.

*4.1.3.2. Phenyl (4-chlorobenzyl)carbamate (**8b**).* Yellowish solid; Yield: 69.8%. MS (ESI) *m/z* (%): 262.8$[M+H]^+$.

*4.1.3.3. Phenyl (2-fluorobenzyl)carbamate (**8c**).* Yellow solid; Yield: 63.4%. MS (ESI) *m/z* (%): 246.4 $[M+H]^+$.

*4.1.3.4. Phenyl (3-fluorobenzyl)carbamate (**8d**).* Yellowish brown solid; Yield: 73.5%. MS (ESI) *m/z* (%): 246.4 $[M+H]^+$.

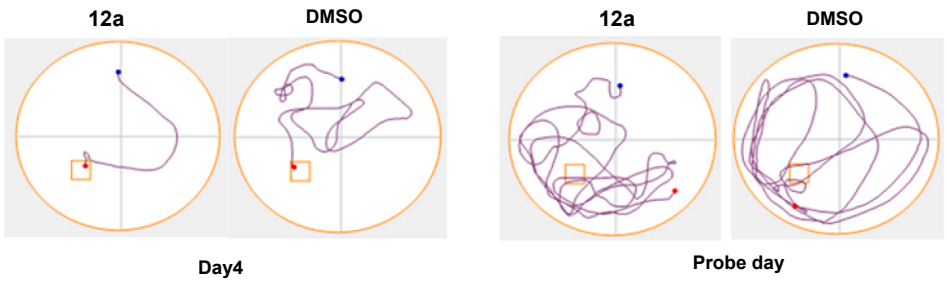

Fig 5. The representative tracks of the mice in Morris water maze during the spatial probe trial period.

*4.1.3.5. Phenyl (4-fluorobenzyl)carbamate (**8e**).* Yellowish solid; Yield: 67.4%. MS (ESI) *m/z* (%): 246.4 $[M+H]^+$.

*4.1.3.6. Phenyl (2,3-dichlorobenzyl)carbamate (**8f**).* Yellow solid; Yield: 66.1%. MS (ESI) *m/z* (%): 297.2 $[M+H]^+$.

*4.1.3.7. Phenyl (2,4-dichlorobenzyl)carbamate (**8g**).* Yellowish brown solid; Yield: 69.7%. MS (ESI) *m/z* (%): 297.2 $[M+H]^+$.

*4.1.3.8. Phenyl (3,4-dichlorobenzyl)carbamate (**8h**).* Yellow solid; Yield: 71.8%. MS (ESI) *m/z* (%): 297.2 $[M+H]^+$.

*4.1.3.9. Phenyl (4-(trifluoromethyl)benzyl)carbamate (**8i**).* Yellowish solid; Yield: 77.6.0%. MS (ESI) *m/z* (%): 296.4 $[M+H]^+$.

*4.1.3.10. Phenyl (4-methylbenzyl)carbamate (**8j**).* Yellow-red solid; Yield: 68.4%. MS (ESI) *m/z* (%): 242.3 $[M+H]^+$.

*4.1.4. General procedure for preparation of hydrazinecarboxamide intermediates (**5a-5l**)*

Substitution phenyl phenylcarbamate (1.2 μmol) and 80% hydrazine hydrate (1.5 μmol) were added into toluene (15 mL). The mixture was heated to 80℃ for 3 h. After being cooled to room temperature, the precipitate was filtered and dried under reduced pressure to afford intermediates ***(5a-5l)***.

*4.1.4.1. N-phenylhydrazinecarboxamide (**5a**).* Pink solid; Yield: 66.3%. MS (ESI) *m/z* (%): 152.3 $[M+H]^+$.

*4.1.4.2. N-(o-tolyl)hydrazinecarboxamide (**5b**).* Light pink solid; Yield: 70.7%. MS (ESI) *m/z* (%): 166.4 $[M+H]^+$.

*4.1.4.3. N-(m-tolyl)hydrazinecarboxamide (**5c**).* Pink solid; Yield: 66.7%. MS (ESI) *m/z* (%): 166.4 $[M+H]^+$.

*4.1.4.4. N-(p-tolyl)hydrazinecarboxamide (**5d**).* Yellow pink solid; Yield: 62.7%. MS (ESI) *m/z* (%): 166.4 $[M+H]^+$.

*4.1.4.5. N-(2-bromophenyl)hydrazinecarboxamide (**5e**).* Pink solid; Yield: 66.7%. MS (ESI) *m/z* (%): 231.1 $[M+H]^+$.

*4.1.4.6. N-(3-bromophenyl)hydrazinecarboxamide (**5f**).* Pink solid; Yield: 62.3%. MS (ESI) *m/z* (%): 231.2 $[M+H]^+$.

*4.1.4.7. N-(4-bromophenyl)hydrazinecarboxamide (**5g**).* Pink solid; Yield: 68.4%. MS (ESI) *m/z* (%): 231.1 $[M+H]^+$.

*4.1.4.8. N-(2-chlorophenyl)hydrazinecarboxamide (**5h**).* Pink solid; Yield: 60.3%. MS (ESI) *m/z* (%): 186.8 $[M+H]^+$.

*4.1.4.9. N-(2-methoxyphenyl)hydrazinecarboxamide (**5i**).* Light pink solid; Yield: 66.3%. MS (ESI) *m/z* (%): 182.4$[M+H]^+$.

*4.1.4.10. N-(2-(trifluoromethoxy)phenyl)hydrazinecarboxamide (**5j**).* Pink solid; Yield: 69.6%. MS (ESI) *m/z* (%):236.3 $[M+H]^+$.

*4.1.4.11. N-(2-(trifluoromethyl)phenyl)hydrazinecarboxamide (**5k**).* Purple and pink solid; Yield: 71.3%. MS (ESI) *m/z* (%): 220.3 $[M+H]^+$.

*4.1.4.12. N-(4-nitrophenyl)hydrazinecarboxamide (**5l**).* Pink solid; Yield: 70.3%. MS (ESI) *m/z* (%): 197.2 $[M+H]^+$.

*4.1.5. General procedure for preparation of hydrazine carboxamide intermediates (**9a-9j**)*

The preparation of the key intermediate **9a-9j** is the same as way to preparation **5a-5l**, so the synthesis method would not be listed here.

*4.1.5.1. N-benzylhydrazinecarboxamide (**9a**).* Pink solid; Yield: 63.3%. MS (ESI) *m/z* (%): 166.4 $[M+H]^+$.

*4.1.5.2. N-(4-chlorobenzyl)hydrazinecarboxamide (**9b**).* Pink solid; Yield: 70.3%. MS (ESI) *m/z* (%): 200.8 $[M+H]^+$.

*4.1.5.3. N-(2-fluorobenzyl)hydrazinecarboxamide (**9c**).* Light pink solid; Yield: 73.3%. MS (ESI) *m/z* (%): 184.4 $[M+H]^+$.

*4.1.5.4. N-(3-fluorobenzyl)hydrazinecarboxamide (**9d**).* Light pink solid; Yield: 70.1%. MS (ESI) *m/z* (%): 184.3 $[M+H]^+$.

*4.1.5.5. N-(4-fluorobenzyl)hydrazinecarboxamide (**9e**).* Pink solid; Yield: 73.3%. MS (ESI) *m/z* (%): 184.4 $[M+H]^+$.

*4.1.5.6. N-(2,3-dichlorobenzyl)hydrazinecarboxamide (**9f**).* Pink solid; Yield: 83.3%. MS (ESI) *m/z* (%): 235.2$[M+H]^+$.

*4.1.5.7. N-(2,4-dichlorobenzyl)hydrazinecarboxamide (**9g**).* Pink yellow solid; Yield: 86.7%. MS (ESI) *m/z* (%): 235.2 $[M+H]^+$.

*4.1.5.8. N-(3,4-dichlorobenzyl)hydrazinecarboxamide (**9h**).* Pink solid; Yield: 80.1%. MS (ESI) *m/z* (%): 235.1$[M+H]^+$.

*4.1.5.9. N-(4-(trifluoromethyl)benzyl)hydrazinecarboxamide (**9i**).* Light pink solid; Yield: 86.6%. MS (ESI) *m/z* (%): 234.3 $[M+H]^+$.

*4.1.5.10. N-(4-methylbenzyl)hydrazinecarboxamide (**9j**).* Pink solid; Yield: 60.3%. MS (ESI) *m/z* (%): 180.4 $[M+H]^+$.

*4.1.6. General procedure for preparation of imidazolyl hydrazide intermediates (**11a-11d**)*

The preparation of the key intermediate **11a-11d** is the same as way to preparation **5a-5l**, so the synthesis method would not be listed here.

*4.1.6.1. 1H-imidazole-5-carbohydrazide (**11a**).* White solid; Yield: 46.3%. MS (ESI) *m/z* (%): 128.1 $[M+H]^+$.

*4.1.6.2. N,1-dimethyl-1H-imidazole-5-carbohydrazide (**11b**).* Grayish white solid; Yield: 39.6%. MS (ESI) *m/z* (%): 155.4 $[M+H]^+$.

*4.1.6.3. 2-bromo-1H-imidazole-5-carbohydrazide (**11c**).* White solid; Yield: 41.2%. MS (ESI) *m/z* (%): 205.3 $[M+H]^+$.

*4.1.6.4. 2-bromo-4-methyl-1H-imidazole-5-carbohydrazide (**11d**).* White solid; Yield: 44.4%. MS (ESI) *m/z* (%): 219.3 $[M+H]^+$.

*4.1.7. General procedure for preparation of target compounds (**6a-6l, 10a-10j, 12a-12d**)*

A mixture of 2(1.5 mmol) and different substituted ***5a-5l, 9a-9j*** or **12a-12d** (1.5 mmol) in EtOH (10 mL) was stirred at for 2 h. the precipitate was filtered and washed with EtOH (5 mL) and dried under reduced pressure to afford compounds ***6a-6l, 10a-10j, 12a-12d*** respectively.

*4.1.7.1. 2-((5-(4-nitrophenyl) furan-2-yl) methylene)-N-phenylhydrazine-1-carboxamide (**6a**).* Yellow solid; Yield: 67.1%; Mp: 239.0–241.3 °C; MS (ESI) *m/z* (%): 349.34 $[M-H]^-$; ^{1}H NMR (600 MHz, DMSO-d_6) δ (ppm): 10.92 (s, 1H, NNHCO), 8.83 (s, 1H, CONHPh), 8.33–8.28 (m, 2H, Ph-H), 8.11–8.05 (m, 2H, Ph-H), 7.93 (s, 1H, N = CH), 7.66 (t, *J* = 7.0 Hz, 2H, Ph-H),7.47(d,*J* = 3.6 Hz, 1H, furan-H), 7.31 (dd, *J* = 8.3, 7.6 Hz, 2H, Ph-H), 7.18 (d, *J* = 3.6 Hz, 1H, furan-H), 7.03 (t, *J* = 7.3 Hz, 1H, Ph-H).

*4.1.7.2. 2-((5-(4-nitrophenyl) furan-2-yl) methylene)-N-(o-tolyl) hydrazine-1-carboxamide (**6b**).* Brown yellow solid; Yield: 74.1%; Mp: 210.1–213.0 °C; MS (ESI) *m/z* (%): 363.20 $[M-H]^-$; ^{1}H NMR (400 MHz, DMSO-d_6) δ (ppm): 10.89 (s, 1H, NNHCO), 8.73 (s, 1H, CONHPh), 8.29 (d, *J* = 8.9 Hz, 2H,Ph-H), 8.06 (d, *J* = 8.8 Hz, 2H, Ph-H), 7.91 (s, 1H, HC = N), 7.53 (d, *J* = 8.3 Hz, 2H, Ph-H), 7.46 (d, *J* = 3.6 Hz, 1H, furan-H), 7.17 (d, *J* = 3.6 Hz, 1H, furan-H), 7.11 (d, *J* = 8.2 Hz, 2H,Ph-H).

*4.1.7.3. 2-((5-(4-nitrophenyl) furan-2-yl) methylene)-N-(m-tolyl) hydrazine-1-carboxamide (**6c**).* Yellow solid; Yield: 74.1%; Mp: 210.4–212.2 °C; MS (ESI) *m/z* (%): 363.20 $[M-H]^-$; ^{1}H NMR (400 MHz, DMSO-d_6) δ (ppm): 10.93 (s, 1H, NNHCO), 8.74 (s, 1H, PhNH), 8.30 (d, *J* = 9.0 Hz, 2H, Ph-H), 8.07 (d, *J* = 8.9 Hz, 2H, Ph-H), 7.92 (s, 1H, N = CH), 7.50 (s, 1H, Ph-H),7.47 (d, *J* = 3.7 Hz, 1H, furan-H), 7.44 (d, *J* = 8.3 Hz, 1H, Ph-H), 7.20 (d, *J* = 3.7 Hz, 1H, furan-H), 7.19 (s, 1H, Ph-H), 6.85(d, *J* = 7.4 Hz, 1H, Ph-H), 2.30 (s, 3H, PhCH3)

*4.1.7.4. 2-((5-(4-nitrophenyl) furan-2-yl) methylene)-N-(p-tolyl) hydrazine-1-carboxamide (**6d**).* Yellow solid; Yield: 77.1%; Mp: 230.6–232.7 °C; MS (ESI) *m/z* (%): 363.26 $[M-H]^-$; HRMS (ESI) *m/z* (%):365.1569 $[M+H]^+$; ^{1}H NMR (400 MHz, DMSO-d_6) δ (ppm): 10.90 (s, 1H, NNHCO), 8.74 (s, 1H, CONHPh), 8.28 (t, *J* = 11.2 Hz, 2H, Ph-H), 8.12–8.03 (m, 2H, Ph-H), 7.92 (s, 1H, HC = N), 7.53 (d, *J* = 8.4 Hz, 2H, Ph-H), 7.46 (dd, *J* = 8.4, 5.6 Hz, 2H, Ph-H), 7.17(d, *J* = 3.6 Hz, 1H, furan-H), 6.75 (d, *J* = 3.6 Hz, 1H,furan-H). ^{13}C NMR (151 MHz, DMSO-d_6) *δ* 169.42, 152.56, 150.55, 146.68, 143.79, 136.51, 135.46, 132.70, 128.84(2C), 124.94(2C), 124.87(2C), 118.96(2C), 116.27, 112.57, 24.49.

*4.1.7.5. N-(2-bromophenyl)-2-((5-(4-nitrophenyl) furan-2-yl) methylene) hydrazine-1-carboxamide (**6e**).* Light yellow solid; Yield: 72.1%; Mp: 250.2–252.8 °C; MS (ESI) *m/z* (%): 427.26 $[M-H]^-$; ^{1}H NMR (400 MHz, DMSO-d_6) δ (ppm): 11.30 (s, 1H, NNHCO), 8.95 (s, 1H, CONHPh), 8.36 (d, *J* = 8.9 Hz, 1H,Ph-H), 8.31 (d, *J* = 8.9 Hz, 2H, Ph-H), 8.24 (d, *J* = 8.2 Hz, 1H, Ph-H), 8.01 (d, *J* = 8.9 Hz, 2H, Ph-H), 7.94 (s, 1H,HC = N), 7.47 (d, *J* = 3.6 Hz, 1H, furan-H), 7.39 (t, *J* = 7.8 Hz, 1H, Ph-H), 7.11 (d, *J* = 3.6 Hz, 1H, furan-H), 7.04 (t, *J* = 7.8 Hz, 1H, Ph-H).

*4.1.7.6. N-(3-bromophenyl)-2-((5-(4-nitrophenyl) furan-2-yl) methylene) hydrazine-1-carboxamide (**6f**).* Yellow solid; Yield: 73.6%; Mp: 252.2–254.1 °C; MS (ESI) *m/z* (%): 427.35 $[M-H]^-$; ^{1}H NMR (400 MHz, DMSO-d_6) δ (ppm): 11.05 (s, 1H,CONHN), 9.05 (s, 1H,PhNH), 8.31 (d, *J* = 8.9 Hz, 2H, Ph-H), 8.08 (d, *J* = 8.8 Hz, 2H, Ph-H), 8.02 (s, 1H, Ph-H), 7.93 (s, 1H ,N = CH), 7.66 (d, *J* = 3.6 Hz, 1H, furan-H), 7.48(d, *J* = 3.6 Hz, 1H,furan-H), 7.20 (s, 1H,Ph-H),7.21 (s, 1H,Ph-H), 7.28 (s, 1H,Ph-H).

*4.1.7.7. N-(4-bromophenyl)-2-((5-(4-nitrophenyl) furan-2-yl) methylene) hydrazine-1-carboxamide (**6g**).* Light yellow solid; Yield: 78.4%; Mp: 251.7–253.4 °C; MS (ESI) *m/z* (%): 427.16 $[M-H]^-$; HRMS (ESI) *m/z* (%): 429.3015$[M+H]^+$; ^{1}H NMR (400 MHz, DMSO-d_6) δ (ppm): 11.01 (s, 1H, NNHCO), 9.02 (s, 1H,CONHPh), 8.31 (d, *J* = 9.0 Hz, 2H,Ph-H), 8.08 (d, *J* = 8.9 Hz, 2H,Ph-H), 7.93 (s, 1H,HC = N), 7.67 (d, *J* = 8.9 Hz,2H, Ph-H), 7.52–7.45 (m, 3H, Ph-H,furan-H), 7.18 (d, *J* = 3.7 Hz,1H, furan-H) . ^{13}C NMR (151 MHz, DMSO-d_6) *δ* 152.60, 150.51, 146.74, 143.98, 136.61(2C), 136.44, 135.46, 130.12(2C), 127.55(2C), 124.97(2C), 124.92(2C), 116.40, 112.61.

*4.1.7.8. N-(2-chlorophenyl)-2-((5-(4-nitrophenyl) furan-2-yl) methylene) hydrazine-1-carboxamide (**6h**).* Yellowish brown solid; Yield: 70.9%; Mp: 210.1–212.5 °C; MS (ESI) *m/z* (%): 383.30 $[M-H]^-$; ^{1}H NMR (400 MHz, DMSO-d_6) δ (ppm): 11.29 (s, 1H,CONHN), 8.96 (s, 1H,PhNHCO), 8.30 (d, *J* = 9.0 Hz, 2H,Ph-H), 8.00 (d, *J* = 9.0 Hz, 2H,Ph-H), 7.93 (s, 1H, CH = N), 7.55 (dd, *J* = 8.0, 1.2 Hz, 1H,Ph-H), 7.46 (d, *J* = 3.6 Hz, 1H, furan-H), 7.35 (s, 1H, Ph-H), 7.33 (s, 1H, Ph-H), 7.10 (s, 1H, Ph-H), 7.09 (d, *J* = 3.6 Hz, 1H, , furan-H).

*4.1.7.9. N-(2-methoxyphenyl)-2-((5-(4-nitrophenyl) furan-2-yl) methylene) hydrazine-1-carboxamide (**6i**).* Yellow solid; Yield: 72.8%; Mp: 231.5–234.1 °C; MS (ESI) *m/z* (%): 379.21 $[M-H]^-$; ^{1}H NMR (600 MHz, DMSO-d_6) δ (ppm): 11.11 (s, 1H, CONHN), 9.67 (s, 1H, CH = N), 8.11 (d, *J* = 8.4 Hz, 2H, Ph-H), 7.99 (d, *J* = 8.3 Hz, 2H, Ph-H), 7.89 (s, 1H, CONHPh), 7.70 (d, *J* = 3.0 Hz, 1H, furan-H), 7.57 (d, *J* = 3.0 Hz, 1H, furan-H), 7.44 (s, 1H, Ph-H), 7.09–6.99 (m, 3H, Ph-H), 3.97 (s, 3H, PhOCH3).

*4.1.7.10. 2-((5-(4-nitrophenyl) furan-2-yl) methylene)-N-(2-(trifluoromethoxy) phenyl) hydrazine-1-carboxamide (**6j**).* Yellow solid; Yield: 79.7%; Mp: 230.0–232.7 °C; MS (ESI) *m/z* (%): 433.27 $[M-H]^-$; ^{1}H NMR (400 MHz, DMSO-d_6) δ (ppm): 11.26 (s, 1H,CONHN), 8.70 (s, 1H,PhNHCO), 8.29(dd, *J* = 14.8, 9.0 Hz, 3H,Ph-H), 8.00 (d, *J* = 9.0 Hz, 2H,Ph-H), 7.93 (s, 1H,CH = N), 7.49–7.36 (m, 4H,furan-H, Ph-H), 7.06 (d, *J* = 3.7 Hz, 1H,furan-H).

*4.1.7.11. 2-((5-(4-nitrophenyl) furan-2-yl) methylene)-N-(2-(trifluoromethyl) phenyl) hydrazine-1-carboxamide (**6k**).* Brown yellow solid; Yield: 79.1%; Mp: 240.2–244.0 °C; MS (ESI) *m/z* (%): 490.46 $[M+Na]^+$; ^{1}H NMR (600 MHz, DMSO-d_6) δ (ppm): 11.36 (s, 1H, CONHN), 8.94 (s, 1H, CH = N), 8.29(d,*J* = 8.9 Hz, 2H, Ph-H), 8.26 (d, *J* = 8.3 Hz, 1H,CONHPh), 8.03 (d, *J* = 8.9 Hz, 2H, Ph-H),7.93 (s, 1H, Ph-H), 7.76–7.68 (m, 2H, Ph-H), 7.48 (d, *J* = 3.6 Hz, 1H, furan-H), 7.31 (t, *J* = 7.6 Hz, 1H, Ph-H), 7.08 (d, *J* = 3.6 Hz, 1H, furan-H)

*4.1.7.12. N-(4-nitrophenyl)-2-((5-(4-nitrophenyl) furan-2-yl) methylene) hydrazine-1-carboxamide (**6l**).* Yellow solid; Yield: 78.4%; Mp: 241.3–234.1 °C; MS (ESI) *m/z* (%): 419.09 $[M+Na]^+$; ^{1}H NMR (400 MHz, DMSO-d_6) δ (ppm): 11.23 (s, 1H,CONHN), 9.55 (s, 1H,PhNHCO), 8.31 (d,*J* = 9.0 Hz, 2H,PhH), 8.22 (d, *J* = 9.3 Hz, 2H,PhH), 8.09 (d, *J* = 8.9 Hz, 2H,PhH), 7.98 (d, *J* = 10.2 Hz, 3H, PhH, N = CH), 7.49 (d, *J* = 3.6 Hz, 1H,furan-H), 7.21 (d, *J* = 3.6 Hz, 1H,furan-H).

4.1.7.13. N-benzyl-2-((5-(4-nitrophenyl) furan-2-yl) methylene) hydrazine-1-carboxamide ***(10a)***. Lightyellowsolid; Yield: 69.2%; Mp:239.2–241.1 °C;MS (ESI) *m/z* (%):366.33[M-H]$^-$; HRMS (ESI) *m/z* (%): 365.1569[M+H]$^+$; ^{1}H NMR (600 MHz, DMSO-d_6) δ (ppm): 10.66 (s, 1H, CONHN), 8.30–8.26 (m, 2H, Ph-H), 8.05–8.00 (m, 2H, Ph-H), 7.85 (s, 1H, CH = N), 7.47 (t, *J* = 6.4 Hz, 1H, CH2NH), 7.43 (d, *J* = 3.6 Hz, 1H, furan-H), 7.37–7.24 (m, 5H, Ph-H), 7.05 (d, *J* = 3.6 Hz, 1H, furan-H), 4.39 (d, *J* = 6.3 Hz, 2H, PhCH2). ^{13}C NMR (151 MHz, DMSO-d_6) *δ* 153.86, 153.29, 150.76, 146.86, 141.27, 139.54, 135.47, 128.69(2C), 128.57, 127.56(2C), 127.36, 127.26, 125.20, 124.81, 117.82, 112.75, 43.84.

4.1.7.14. N-(4-chlorobenzyl)-2-((5-(4-nitrophenyl) furan-2-yl) methylene) hydrazine-1-carboxamide ***(10b)***. Yellowish brown solid; Yield: 80.1%; Mp: 211.6–215.4 °C; MS (ESI) *m/z* (%): 397.16 [M−H]$^-$; ^{1}H NMR (600 MHz, DMSO-d_6) δ (ppm): 10.69 (s, 1H, CONHN), 8.29–8.27 (m, 2H, Ph-H), 8.04–8.02 (m, 2H, Ph-H), 7.84 (s, 1H, CH = N), 7.44 (d, *J* = 3.6 Hz, 1H, furan-H), 7.40 (d, *J* = 1.8 Hz, 1H, CH2NH), 7.36 (dd, *J* = 29.8, 5.3 Hz, 4H, Ph-H), 7.05 (d, *J* = 3.6 Hz, 1H,furan-H), 4.36 (d, *J* = 6.3 Hz, 2H, PhCH2).

4.1.7.15. N-(2-fluorobenzyl)-2-((5-(4-nitrophenyl) furan-2-yl) methylene) hydrazine-1-carboxamide ***(10c)***. Yellow solid; Yield: 77.5%; Mp: 221.3–222.8 °C; MS (ESI) *m/z* (%): 381.29 [M-H]$^-$; ^{1}H NMR (400 MHz, DMSO-d_6) δ (ppm): 10.71 (s, 1H,CONHN), 9.68 (s, 1H,CH = N), 8.27 (d, *J* = 9.1 Hz, 2H,Ph-H), 8.02 (d, *J* = 9.0 Hz, 2H,Ph-H), 7.85 (s, 1H, CONHCH2), 7.46 (d, *J* = 3.9 Hz, 1H,Ph-H), 7.43 (d, *J* = 3.7 Hz, 1H, furan-H), 7.36 (t, *J* = 7.6 Hz, 1H,Ph-H), 7.29 (ddd, *J* = 9.4, 7.5, 1.6 Hz, 1H,Ph-H), 7.15–7.09 (m, 1H,Ph-H), 7.05 (d, *J* = 3.7 Hz, 1H,furan-H), 4.44 (d, *J* = 6.2 Hz, 2H,PhCH2NH).

4.1.7.16. N-(3-fluorobenzyl)-2-((5-(4-nitrophenyl) furan-2-yl) methylene) hydrazine-1-carboxamide ***(10d)***. Yellow solid; Yield: 78.7%; Mp: 222.3–224.4 °C; MS (ESI) *m/z* (%): 381.29 [M−H]$^-$; ^{1}H NMR (400 MHz, DMSO-d_6) δ (ppm): 10.69 (s, 1H, CONHN), 8.27 (d, *J* = 9.0 Hz, 2H, Ph-H), 8.03 (d, *J* = 9.0 Hz, 2H, Ph-H), 7.85 (s, 1H, CH = N), 7.57 (dd, *J* = 12.1, 5.7 Hz, 1H, Ph-H),7.43 (d, *J* = 3.6 Hz, 1H, furan-H), 7.36 (dd, *J* = 7.8, 6.3 Hz, 1H, CH2NH), 7.19–7.06 (m, 3H,Ph-H), 7.05 (d, *J* = 3.6 Hz, 1H, furan-H), 4.40 (d, *J* = 6.3 Hz, 2H, PhCH2).

4.1.7.17. N-(4-fluorobenzyl)-2-((5-(4-nitrophenyl) furan-2-yl) methylene) hydrazine-1-carboxamide ***(10e)***. Yellowish brown solid; Yield: 77.6%; Mp: 224.8–226.1 °C; MS (ESI) *m/z* (%): 381.29 [M-H]$^-$; ^{1}H NMR (400 MHz, DMSO-d_6) δ (ppm): 10.69 (s, 1H, CONHN), 8.29–8.27 (m, 2H, Ph-H),8.04–8.02 (m, 2H, Ph-H), 7.84 (s, 1H, CH = N), 7.38–7.32 (m, 2H, Ph-H),7.12–7.07 (m, 2H,Ph-H), 6.96 (d, *J* = 3.6 Hz, 1H, furan-H), 6.64 (d, *J* = 3.6 Hz, 1H, furan-H), 6.12 (s, 1H, CH2NH), 4.36(d,*J* = 6.3 Hz,2H, PhCH2).

4.1.7.18. N-(2,3-dichlorobenzyl)-2-((5-(4-nitrophenyl) furan-2-yl) methylene) hydrazine-1-carboxamide ***(10f)***. Yellow solid; Yield: 81.1%; Mp: 226.1–229.5 °C; MS (ESI) *m/z* (%): 433.40 [M+H]$^+$; ^{1}H NMR (600 MHz, DMSO-d_6) δ (ppm): 10.80(s, 1H, CONHN), 8.28 (d, *J* = 8.8 Hz, 2H, Ph-H), 8.04 (d, *J* = 8.6 Hz, 2H, Ph-H), 7.87 (s, 1H, CH = N), 7.61 (s, 1H, CH2NH), 7.45 (d,*J* = 3.5 Hz, 1H, furan-H),7.42–7.28 (m, 3H, Ph-H), 7.06 (d, *J* = 3.5 Hz, 1H, furan-H), 4.48 (d, *J* = 5.9 Hz, 2H, PhCH2).

4.1.7.19. N-(2,4-dichlorobenzyl)-2-((5-(4-nitrophenyl) furan-2-yl) methylene) hydrazine-1-carboxamide ***(10g)***. Yellow solid; Yield: 83.1%; Mp: 223.4–225.8 °C; MS (ESI) *m/z* (%): 433.33 [M+H]$^+$; ^{1}H NMR (600 MHz, DMSO-d_6) δ (ppm): 10.79 (s, 1H, CONHN), 8.28 (d, *J* = 8.9 Hz, 2H, Ph-H),8.03 (d, *J* = 8.9 Hz, 2H, Ph-H), 7.95 (s, 1H, CH = N), 7.87 (s, 1H, Ph-H), 7.62 (d, *J* = 2.0 Hz,2H, Ph-H), 7.44 (s, 1H, CH2NH), 7.35 (d, *J* = 3.6 Hz, 1H, furan-H), 7.06 (d, *J* = 3.6 Hz, 1H, furan-H), 4.42 (d, *J* = 6.1 Hz, 2H, PhCH2).

4.1.7.20. N-(3,4-dichlorobenzyl)-2-((5-(4-nitrophenyl) furan-2-yl) methylene) hydrazine-1-carboxamide ***(10h)***. Yellow solid; Yield: 82.3%; Mp: 221.4–224.0 °C; MS (ESI) *m/z* (%): 431.19 [M−H]$^-$; ^{1}H NMR (600 MHz, DMSO-d_6) δ (ppm): 10.72 (s, 1H, CONHN), 8.28 (d, *J* = 8.7 Hz, 2H, Ph-H),8.03 (d, *J* = 8.7 Hz, 2H, Ph-H), 7.85 (s, 1H, CH = N), 7.63–7.54 (m, 3H, Ph-H), 7.44 (d, *J* = 3.4 Hz, 1H, furan-H), 7.31 (d, *J* = 8.0 Hz, 1H, CH2NH), 7.05 (d, *J* = 3.4 Hz, 1H, furan-H),4.36 (d, *J* = 6.1 Hz, 2H, PhCH2).

4.1.7.21. 2-((5-(4-nitrophenyl) furan-2-yl) methylene)-N-(4-(trifluoromethyl) benzyl) hydrazine-1-carboxamide ***(10i)***. Light yellow solid; Yield: 87.4%; Mp: 208.9–210.7 °C; MS (ESI) *m/z*(%): 431.25 [M-H]$^-$; ^{1}H NMR (600 MHz, DMSO-d_6) δ (ppm): 10.72 (s, 1H, CONHN), 8.29 (d, *J* = 2.0 Hz, 2H, Ph-H),8.04 (d, *J* = 1.8 Hz, 2H, Ph-H), 7.85 (s, 1H, CH = N), 7.60 (d, *J* = 4.2 Hz, 2H, Ph-H), 7.59 (s,1H, CH2NH), 7.54 (d, *J* = 4.0 Hz, 2H, Ph-H), 7.44 (d, *J* = 2.1 Hz, 1H, furan-H), 7.05 (d, *J* = 2.1 Hz, 1H, furan-H), 4.36 (d, *J* = 6.3 Hz, 2H, PhCH2).

4.1.7.22. N-(4-methylbenzyl)-2-((5-(4-nitrophenyl) furan-2-yl) methylene) hydrazine-1-carboxamide ***(10j)***. Brown yellow solid; Yield: 68.4%; Mp: 231.5–233.6 °C; MS (ESI) *m/z*(%): 377.32 [M−H]$^-$; ^{1}H NMR (600 MHz, DMSO-d_6) δ (ppm): 10.65 (s, 1H, CONHN), 8.28 (d, *J* = 8.8 Hz, 2H, Ph-H),8.03 (d, *J* = 8.8 Hz, 2H, Ph-H), 7.83 (s, 1H, CH = N), 7.44 (d, *J* = 3.6 Hz, 1H, furan-H), 7.21–7.14 (m, 4H, Ph-H), 7.13 (s, 1H, CH2NH), 7.04 (d, *J* = 3.6 Hz, 1H, furan-H), 4.33 (d, *J* = 6.2 Hz, 2H, PhCH2), 2.27 (s, 3H, PhCH3).

4.1.7.23. N'-((5-(4-nitrophenyl) furan-2-yl) methylene)-1H-imidazole-5-carbohydrazide ***(12a)***. Light yellow solid; Yield: 78.4%; Mp: 261.9–262.8 °C; MS (ESI) *m/z* (%): 326.4 [M+H]$^+$; HRMS (ESI) *m/z* (%): 348.0710[M+Na]$^+$; ^{1}H NMR (400 MHz, DMSO-d_6) δ (ppm): 12.69 (s, 1H, Imidazole-NH), 11.71 (s, 1H,NNHCO), 8.51 (s, 1H, CH = N), 8.32 (d, *J* = 8.9 Hz, 2H, Ph-H), 8.03 (d, *J* = 8.9 Hz, 2H, Ph-H), 7.86 (s, 1H, NCHN–), 7.85 (s, 1H,C = CH-N), 7.47 (d, *J* = 3.6 Hz, 1H, furan-H), 7.07 (d, *J* = 3.6 Hz, 1H, furan-H). ^{13}C NMR (151 MHz, DMSO-d_6) *δ* 152.50, 151.85, 146.61(2C), 136.40, 135.64(2C), 125.69, 124.92(4C), 115.72, 112.89(2C).

4.1.7.24. N,1-dimethyl-N'-((5-(4-nitrophenyl)furan-2-yl)methylene)-1H-imidazole-5carbohydrazide ***(12b)***. yellow solid; Yield: 79.2%; Mp: 258.9–262.7 °C;MS (ESI) *m/z*(%): 354.2 [M+H]$^+$; ^{1}H NMR (400 MHz, DMSO-d_6) δ (ppm): 8.35 (d, *J* = 8.6 Hz, 2H, Ph-H), 8.27 (s, 1H, CH = N), 8.06 (d, *J* = 8.6 Hz, 2H, Ph-H), 7.98 (s, 1H, Imidazole-N = CH), 7.75 (s, 1H, Imidazole-C = CH), 7.50 (d, *J* = 3.5 Hz, 1H, furan-H), 7.07 (d, *J* = 3.8 Hz, 1H, furan-H), 3.51 (s, 3H,–CH3), 3.44 (s, 3H, Imidazole-CH3).

4.1.7.25. 2-bromo-N'-((5-(4-nitrophenyl) furan-2-yl) methylene)-1H-imidazole-5-carbohydrazide ***(12c)***. Light yellow solid; Yield: 81.3%; Mp: 256.8–259.7 °C;MS (ESI) *m/z*(%): 348.46 [M+Na]$^+$;^{1}H NMR (600 MHz, DMSO-d_6) δ (ppm): 13.79 (s, 1H, Imidazole-NH), 12.31 (s, 1H,NH), 8.53 (s, 1H, CH = N), 8.32 (d, *J* = 8.9 Hz, 2H, Ph-H), 8.05 (d, *J* = 8.9 Hz, 2H, Ph-H), 7.59 (s, 1H,*N*-CH = C), 7.49 (d, *J* = 3.6 Hz, 1H, furan-H), 7.14 (d, *J* = 3.7 Hz, 1H, furan-H).

4.1.7.26. 2-bromo-4-methyl-N'-((5-(4-nitrophenyl) furan-2-yl) methylene)-1H-imidazole-5-carbohydrazide ***(12d)***. Yellow solid; Yield: 77.6%; Mp:254.9–257.7℃; MS(ESI)*m/z*(%): 340.33[M+H]$^+$; HRMS(ESI)*m/z* (%):362.0903[M+Na]$^+$; ^{1}H NMR (600 MHz, DMSO-d_6) δ (ppm): 13.39 (s, 1H, Imidazole-NH), 11.81 (s, 1H,–NH), 8.48 (s, 1H, CH = N), 8.39 (d, *J* = 8.9 Hz, 2H, Ph-H), 8.34 (d, *J* = 8.9 Hz, 2H, Ph-H), 7.61 (d, *J* = 3.8 Hz, 1H, furan-H), 7.21 (d, *J* = 3.8 Hz, 1H, furan-H), 2.52 (s, 3H,CH3).

4.2. Pharmacology

4.2.1. In vitro SOICR inhibition activities assay

The method was as follows: after induced by 1 mg/ml tetracycline, the cells grew on glass cover slides for 20–24 h, then loaded with fluorescent calcium indicator dye (fura-2AM, 5 mM) in KRH buffer (125 mm NaH_2PO_4 1.2 mm glucose, 1.2 mM $MgCl_2$ and 25 mm HEPES Ph7.35–7.45) and kept at room temperature for 20 min. The cover slides were installed in the perfusion chamber, and different concentrations of $CaCl_2$, were infused into the KRH solution to gradually increase the calcium concentration from 0.1, 0.5 to 1 mM. Then the cells were continuously perfused with KRH solution containing 1 mM $CaCl_2$, and the concentration of the tested compound (0.1 μM, 3 μM, 10 μM) was gradually increased for 8 min each time. Caffeine (10 mM) was applied at the end of each experiment to verify that functional RyR1 channels did exist in the cells.

At the end of the experiment, the delayed image (0.25 frame/s) was captured by the microscope, and the cells with calcium oscillation signal and calcium oscillation peak after adding caffeine were selected for statistics. The number of cells without calcium oscillation signal in different concentration time range was recorded and calculated according to the following formula: Inhibition rate = the number of cells without calcium oscillation signal/the total number of cells * 100%.

4.2.2. Morris water maze test

The Morris water maze test was used to evaluate the learning and memory abilities of the animal models in terms of spatial position and direction (spatial orientation). For the experiment proper, 5-month-old SPF-grade FAD mice, male and female, were randomly selected as our study subjects, and the experiment began 30 days after administration. The animal subjects in the experiment were divided into two groups (six mice per group): the experimental group was injected intraperitoneally with a 3.2 mg/kg 12a DMSO solution (1.12 mg/ml), and the control group was similarly injected with the same volume of DMSO.

Choose a quiet, dim light, constant temperature environment for testing, the laboratory walls can be appropriately affixed with different graphics to help animals determine the location. Before the experiment, the bucket was filled with clear water to a predetermined height (about 40 cm), then an appropriate amount of milk powder was added to make the water an opaque milky liquid, and the heater heated the water to 25℃. The platform is located in the center of southwest quadrant, about 1.5 cm below the water surface, and the position of the platform remains unchanged throughout the experiment. During the training period, the animals were put into the water facing the pool wall from four entry points in turn, and the time required for the animals to find and climb onto the platform was recorded, that is, the escape incubation period, and stayed for 5 s for training in the next direction (by observing the surrounding environment to locate themselves). If the platform is not found within 60 s, the experimenter will lead it to the platform and stay on the platform for 20 s and then train in the next direction. The first 4 days is the animal training period. The positioning navigation experiment is used to evaluate the learning and memory ability of animals. On the 5th day, the platform was removed, and the animals were placed into the water facing the pool wall from the north point. The swimming time in the target quadrant (the southwest quadrant) was recorded.

4.2.3. Statistical analysis

The Pharmacology section statistics were dealt with GraphPad Prism software (GraphPad, Software, Version 6, USA). The effects of the tested drug were analyzed with one way ANOVA followed by T- test of mean values or one-way analysis of variance followed by Dunnett's test. Data are expressed as mean ± SD. Value of $p < 0.05$ was used to express statistically significant difference.

4.2.4. AChE inhibition experiments

AChE inhibitory activity was measured with 96-well plates using the spectrophotometric method. Compounds 6a, 6b, 10d, 10 g, 12a, and 12b were dissolved in DMSO solution. In a final volume of 250 μL of DMSO, 60 μM of Ellman's reagent or 5,5′-dithiobis(2-nitrobenzoic acid), 0.05 M of pH 8 phosphate buffer, 100 μM of inhibitors, and 0.25 U/mL of AChE from E. electricus were incubated for 30 min; then, 1.5 mM of acetylthiocholine iodide was added to start the reaction. The assay was carried out in three experiments in triplicate and absorbance was measured at 412 nm for 10 min. The percentage of inhibition was calculated by comparing the mice's enzyme reaction rates with those of the control group. Donepezil was used as a positive control.

4.2.5. Aqueous solubility assay

The kinetic water solubility of each tested compound was measured using a turbidimetric assay via Cyprotex (Watertown, MA). Each test compound was prepared as a 100-X concentrated stock solution in DMSO, from which serial dilutions were performed to yield eight solutions with final test compound concentrations of 1.6, 3.21, 6.25, 12.5, 25, 50, 100, and 200 mM. Each test compound solution was introduced into a 96-well plate, diluted 100-fold with PBS buffer (pH 7.4), and mixed. The solutions were incubated for two h, and absorbance was measured at 540 nm. An absorbance value > 3X standard deviation of the average blank absorption value was considered to exhibit turbidity. The highest test compound concentration with no sign of turbidity was indicative of a compound's kinetic water solubility.

4.2.6. Molecular docking

The molecular docking procedure was performed by using C-DOCKER protocol within Accelrys Discovery Studio Visualizer 4.0. The RyR1 models was built using PDB code: 6M7H as template. The protein coordinates were downloaded from the Protein Data Bank (http://www.rcsb.org/pdb/). For enzyme preparation, the hydrogen atoms were added. The whole RyR1 enzyme was defined as a receptor and the site sphere was selected on the basis of the ligand binding location of initial ligand. The initial ligand was removed and compound 12a and Dantrolene were placed. Accelrys Discovery Studio Visualizer 4.0 was used for graphic display.

Declaration of Competing Interest

The authors declare that they have no known competing financial interests or personal relationships that could have appeared to influence the work reported in this paper.

Acknowledgements

This work was supported by the Program for Innovative Research Teams by the Ministry of Education of the People's Republic of China and the Program for Liaoning Innovative Research Team in University (IRT1073), Liaoning XingLiao Talents Program (XLYC1807093), the Student's Platform for Innovation and Entrepreneurship Training Program of Shenyang Pharmaceutical University, and S.R. Wayne Chen's lab in University of Calgary.

References

1 Reitz C, Mayeux RJBp: Alzheimer disease: epidemiology, diagnostic criteria, risk factors and biomarkers. 2014;88(4):640–651.
2 Pistollato F, Ohayon E, Lam A et al. Alzheimer disease research in the 21st century: past and current failures, new perspectives and funding priorities. 2016;7(26): 38999–39016.
3 Pender RJA, Association DtJotA: World Alzheimer Report 2014 Dementia and Risk Reduction. 2014;11(7):P837–P837.
4 Xu J, Begley P, Church S et al. Graded perturbations of metabolism in multiple regions of human brain in Alzheimer's disease: Snapshot of a pervasive metabolic disorder. 2016;1862(6):1084–1092.
5 Liu P, Fleete M, Jing Y, et al. Altered arginine metabolism in Alzheimer's disease brains. 2014;35(9):1992–2003.
6 Inoue K, Tsutsui H, Akatsu H, Hashizume Y, Matsukawa N, Yamamoto T, Toyo'oka TJSr: Metabolic profiling of Alzheimer's disease brains. 2013;3:2364.

7 Morrison LD, Smith DD, Kish SJJJoN: Brain S-adenosylmethionine levels are severely decreased in Alzheimer's disease. 2010;67(3):1328–1331.
8 Wang X, Sun G, Feng T et al. Sodium oligomannate therapeutically remodels gut microbiota and suppresses gut bacterial amino acids-shaped neuroinflammation to inhibit Alzheimer's disease progression. 2019;29(10):787–803.
9 Ritter JJBjocp: Drugs for Alzheimer's disease. 2012;73(4):501–503.
10 Birks J, Harvey RJTCdosr: Donepezil for dementia due to Alzheimer's disease. 2003 (3):CD001190.
11 Haass C, Selkoe DJNrMcb: Soluble protein oligomers in neurodegeneration: lessons from the Alzheimer's amyloid beta-peptide. 2007;8(2):101–112.
12 Poorkaj P, Kas A, D'Souza I, et al. A genomic sequence analysis of the mouse and human microtubule-associated protein tau. 2001;12(9):700–712.
13 Inhibition of protein phosphatases induces transport deficits and axonopathy %J Journal of Neurochemistry. 2010;102(3):878–886.
14 Zhou L, McInnes J, Wierda K et al. Tau association with synaptic vesicles causes presynaptic dysfunction 2017;8:15295.
15 Sasaki AJNojotJSoN: Microglia and brain macrophages: An update. 2017;37(5): 452–464.
16 Rosenberg P, Nowrangi M, Lyketsos CJMaom: Neuropsychiatric symptoms in Alzheimer's disease: What might be associated brain circuits? 2015:25–37.
17 Brian J, Alzheimers BJ. Dementia: Calcium dysregulation in Alzheimer's disease; 2009.
18 Popugaeva E, Pchitskaya E, Bezprozvanny IJB, communications br: Dysregulation of neuronal calcium homeostasis in Alzheimer's disease – A therapeutic opportunity? 2017;483(4):998–1004.
19 Bojarski L, Herms J, Kuznicki JJNi: Calcium dysregulation in Alzheimer's disease. 2008;52:621–633.
20 Brawek B, Garaschuk OJC, research t: Network-wide dysregulation of calcium homeostasis in Alzheimer's disease. 2014;357(2):427–438.
21 Fill M, Copello JJPr: Ryanodine receptor calcium release channels. 2002;82(4): 893–922.
22 Bers DJN: Cardiac excitation-contraction coupling 2002;415(6868):198–205.
23 Van Petegem FJJomb: Ryanodine receptors: allosteric ion channel giants. 2015;427 (1):31–53.
24 Yang L, Tautz T, Zhang S, et al. The current status of malignant hyperthermia. 2019; 34(2):75–85.
25 Bolognino I, Giangregorio N, Pisani L et al. A prospective repurposing of dantrolene as a multitarget agent for Alzheimer's disease. 2019;24(23).
26 Chen W, Koop A, Liu Y et al. Reduced threshold for store overload-induced Ca release is a common defect of RyR1 mutations associated with malignant hyperthermia and central core disease. 2017;474(16):2749–2761.
27 De Leiris J, Feuvray DJCr: Factors affecting the release of lactate dehydrogenase from isolated rat heart after calcium and magnesium free perfusions 1973;7(3):383–390.
28 Peng J, Liang G, Inan S et al. Dantrolene ameliorates cognitive decline and neuropathology in Alzheimer triple transgenic mice. 2012;516(2):274–279.
29 Chakroborty S, Briggs C, Miller M et al. Stabilizing ER Ca2+ channel function as an early preventative strategy for Alzheimer's disease. 2012;7(12):e52056.
30 Brandom BW, Green LM, Alvin MS et al. Complications Associated With the Administration of Dantrolene 1987 to 2006. 2011.
31 Krause J, Chenard BJAotNYAoS: Opportunities and challenges in the discovery of new central nervous system drugs. 2008;1144:243–250.
32 Aoyama H, Doura TJB, letters mc: Selective acetylcholinesterase inhibitors derived from muscle relaxant dantrolene. 2020;30(4):126888.
33 N'Da C, Petzer A, Petzer JJDr. The inhibition of acetylcholinesterase by dantrolene and ondansetron. 2015, 65(1):46–51.
34 Ellman GL, Courtney KD, Andres V, Featherstone RM. A new and rapid colorimetric determination of acetylcholinesterase activity. *Biochem Pharmacol.* 1961;7(2):88–95.
35 Wager T, Chandrasekaran R, Hou X et al. Defining desirable central nervous system drug space through the alignment of molecular properties, in vitro ADME, and safety attributes. 2010;1(6):420–434.
36 Bromley-Brits K, Deng Y, Song WJJoveJ: Morris water maze test for learning and memory deficits in Alzheimer's disease model mice 2011(53).